AMERICAN ACADEMY OF OPHTHALMOLOGY®

Cotransplantation of Limbal Epithelial and Stromal Cells for Ocular Surface Reconstruction

Liqiong Zhu, PhD, Wang Zhang, MD,* Jin Zhu, MS,* Chaoqun Chen, BS, Kunlun Mo, BS, Huizhen Guo, MS, Siqi Wu, BS, Huaxing Huang, MS, Lingyu Li, MS, Mingsen Li, PhD, Jieying Tan, BS, Ying Huang, BS, Li Wang, PhD, Hong Ouyang, PhD*

Purpose: To propose an improved stem cell-based strategy for limbal stem cell deficiency (LSCD) treatment.
Design: Experimental randomized or parallel-group animal study.
Subjects: Fifty adult male New Zealand white rabbits.
Methods: Human limbal stem/progenitor cells (LSCs) and limbal stromal stem/progenitor cells (LSSCs) were cultured in serum-free conditions and further differentiated into corneal epithelial cells and keratocytes, respectively. All cell types were characterized with lineage-specific markers. Gene expression analysis was performed to identify the potential function of LSSCs in corneal regeneration. Two LSCD models of rabbits for transplantations were used: transplantation performed at the time of limbal and corneal epithelial excision (LSCD model) and transplantation performed after clinical signs were induced in an LSCD model (pLSCD model). The pLSCD model better mimics the pathologic changes and symptoms of human LSCD. Rabbit models received LSC or LSC plus LSSC treatment. Corneal epithelial defects, neovascularization, and opacity were assessed every 3 weeks for 24 weeks. ZsGreen-labeled LSSCs were used for short-term tracking in vivo.
Main Outcome Measures: Rates of corneal epithelial defect area, corneal neovascularization and opacity scores, graft survival rate, and immunofluorescence staining of specific markers.
Results: Both LSC transplantation and LSC plus LSSC cotransplantation effectively repaired the corneal surface in the LSCD model. These 2 strategies showed no significant differences in terms of graft survival rate or epithelial repair. However, corneal opacity was observed in the LSC group (in 3 of 8 rabbits), but not in the LSC plus LSSC group. Notably, when treating LSCD rabbits with distinguishable stromal opacification and neovascularization, cotransplantation of LSCs and LSSCs exhibited significantly better therapeutic effects than transplantation of LSCs alone, with graft survival rates of 87.5% and 37.5%, respectively. The implanted LSSCs could differentiate into keratocytes during the wound-healing process. RNA sequencing analysis showed that the stromal cells produced not only a collagen-rich extracellular matrix to facilitate reconstruction of the lamellar structure, but also niche factors that accelerated epithelial cell growth and inhibited angiogenesis and inflammation.
Conclusions: These findings highlight the support of stromal cells in niche homeostasis and tissue regeneration, providing LSC plus LSSC cotransplantation as a new treatment strategy for corneal blindness. *Ophthalmology Science 2022;2:100148 © 2022 by the American Academy of Ophthalmology. This is an open access article under the CC BY-NC-ND license (http://creativecommons.org/licenses/by-nc-nd/4.0/).*

Supplemental material available at www.ophthalmologyscience.org.

The cornea protects the eye from external elements, supplies most of the optical power, and enables light refraction. The transparency of the cornea largely depends on epithelial integrity and highly organized stromal fibers. Given its exposure to various insults, the corneal epithelium is continuously replenished throughout the lifespan by limbal stem/progenitor cells (LSCs) residing in the limbus.[1] However, severe corneal trauma, such as inflammation, chemical burns, and infections, may cause LSC deficiency (LSCD) and neovascularization, leading to visual impairment and blindness in millions of individuals worldwide.[2] Transplantation of cultured autologous LSCs has shown great potential as a clinical treatment for reconstruction of the corneal epithelium and limbal barrier in patients with LSCD.[3] However, the unsatisfactory success rate of transplantation in terms of postoperative visual acuity necessitates improved strategies.

Mounting evidence suggests that the interactions between epithelial cells and adjacent stromal cells are essential for tissue development, homeostasis, and

https://doi.org/10.1016/j.xops.2022.100148
ISSN 2666-9145/22

regeneration.[4] Hedgehog-responsive mesenchymal cells beneath the intestinal epithelium control the formation of intestinal villi.[5] Bone morphogenetic protein and Wnt signaling establish different microniches at epithelial mesenchymal cell interfaces during wound healing, helping to precisely orchestrate the heterogeneity of stem cells and transit-amplifying hair follicle cells.[6] Soluble cytokines, hepatocyte growth factor (HGF), and keratinocyte growth factor are produced in keratocytes and regulate epithelial cell proliferation and differentiation.[7] Likewise, the corneal epithelium releases interleukin 1 to induce keratocytes apoptosis in response to injury.[8]

The corneal stroma comprises sparsely embedded keratocytes and uniformly arranged collagen fibrils, which comprise 90% of the corneal volume.[9] Keratocytes are responsible for maintaining the unique stromal structure by secreting collagens and proteoglycans.[10] Unlike the rapid turnover of corneal epithelial cells (CECs), keratocytes are normally quiescent.[11] However, in response to corneal injury, especially that causing disruption of the basement membrane, keratocytes can become activated and transform into fibroblasts, thereby forming stromal fibrosis and scar tissue and resulting in impaired vision.[12] Although keratoplasty is widely used to replace the diseased cornea, the supply of donor corneas is significantly short, meeting only one-seventieth of the global need.[13] Tissue engineering approaches have been developed in an effort to construct artificial corneas with biomaterials, such as hydrogel-based scaffolds and gelatin nanofibers.[14] Biosynthetic implants made from recombinant human collagen are low risk.[15] Recently, a population of stromal stem cells expanded from human limbal biopsy tissue demonstrated similar properties to those of mesenchymal stem cells.[16] These limbal biopsy-derived stromal cells can form spheres expressing neural stem or progenitor cell markers (NESTIN, PAX6, and SOX2), can differentiate into keratocytes, and can prevent corneal scarring in healing wounds,[17] indicating their clinical potential for treating damaged stromal tissue.

Herein, based on pathologic findings showing that LSCD is accompanied by severe stromal destruction, we aimed to reconstruct both the corneal epithelium and stroma in damaged corneas. To eliminate the risk of xenogeneic contamination, we established serum-free expansion and differentiation systems for LSCs and limbal stromal stem/progenitor cells (LSSCs). To evaluate their therapeutic effects, LSCs were used alone or in combination with LSSCs in rabbit models of LSCD. By comparing fibroblasts cultivated from diseased corneas, we further explored the potential contribution of stromal cells to corneal regeneration.

Methods

Human Samples

All human corneal tissues were obtained from the eye bank (Zhongshan Ophthalmic Center, Sun Yat-sen University, Guangzhou, China) with the approval of the Ethics Committee of Zhongshan Ophthalmic Center of Sun Yat-sen University. The research adhered to the tenets of the Declaration of Helsinki.

Isolation and Culture of Limbal Stem/Progenitor Cells and Limbal Stromal Stem/Progenitor Cells

Limbal tissues were isolated from donor and incubated in dispase II (10 mg/ml) for 1 hour at 37 °C, and then surgically separated into epithelial and stromal tissue under a stereo microscope. The dissected epithelium was then cut into pieces and incubated with 0.2% type IV collagenase solution (Gibco) at 37 °C for 2 hours and further digested with 0.25% trypsin-EDTA (Gibco) at 37 °C for 15 minutes. The epithelial cells were seeded on 12-well polystyrene plates (Corning) coated with 2% Matrigel (BD Biosciences). The serum-free medium for LSCs included DMEM/F12 (Gibco) and DMEM (Gibco; 1:1) with 1% penicillin/streptomycin (Gibco), 10 ng/ml EGF (Millipore), 10 μg/ml insulin, 10^{-9} M 3,3′,5-triiodo-L-thyronine, 0.2 μg/ml hydrocortisone (Millipore), 0.1 nM cholera toxin, 10^{-9} M manganese sulfate monohydrate, 6×10^{-7} M sodium selenite, 5×10^{-4} M sodium metasilicate, 5×10^{-6} M ammonium metavanadate, 5×10^{-10} M nickel chloride hexahydrate, 5×10^{-10} M stannous chloride dihydrate, 5×10^{-7} M ethanolamine, 5×10^{-6} M O-phosphorylethanolamine, 3×10^{-9} M ammonium molybdate tetrahydrate, 5 g/l 4-(2-hydroxyethyl) piperazine-1-ethanesulfonic acid, 30 μg/ml L-ascorbic acid 2-phosphate sesquimagnesium salt hydrate, 2% of a bovine serum albumin, 1% of a chemically defined lipid concentrate (ThermoFisher), and 10% of a knockout serum replacement (Gibco). All reagents were purchased from Sigma-Aldrich, unless otherwise noted. The reagents used in this study are shown in Table S1.

The stromal tissues were cut into pieces and incubated with 0.5 mg/ml type L collagenase overnight at 37°C. Cell suspension was then seeded on 24-well polystyrene plates (Corning) coated with 30 μg/ml collagen I (Gibco). The ingredients of LSSCs culture medium were as follows: low-glucose DMEM (Gibco) and MCDB-201 (3:2) with 50 μg/ml gentamicin, 1 × insulin-transferrin-selenium (Gibco), 20 ng/ml EGF, 0.1 mM L-ascorbic acid 2-phosphate sesquimagnesium salt hydrate, 10^{-8} M dexamethasone, and 100 ng/ml cholera toxin. Fibroblasts derived from donor tissue of patients with LSCD were cultured in medium of DMEM with 2% fetal bovine serum.

Air–Liquid Interface Culture System

Limbal stem/progenitor cells were seeded on collagen I-coated transwell plates (Corning) as 2×10^4 cells/insert and were cultured with LSC medium. When cell confluence reached 100%, the medium inside the inserts was removed, and the lower compartment remained 200 μl medium (changed every day) for an additional 5 to 8 days to obtain mature CECs.

In Vitro Differentiation of Limbal Stromal Stem/Progenitor Cells into Keratocytes

Limbal stromal stem/progenitor cells were maintained in the following medium for 1 week: low-glucose DMEM, 1 × insulin-transferrin-selenium, 1 mM L-ascorbic acid 2-phosphate sesquimagnesium salt hydrate, 100 ng/ml bFGF (R&D), 2 mM L-glutamine (Gibco), and 50 μg/ml gentamicin. The medium was changed every day.

Lentiviral Vectors and Infection

PLVX-ZsGreen-IRES-Puro lentiviral vector (Addgene) was used to generate green fluorescent protein. Limbal stromal stem/progenitor cells were infected according to the lentiparticles application guide for 16 to 20 hours in the presence of 8 μg/ml polybrene. For further selection, the infected cells were exposed to 2 μg/ml puromycin for 48 hours.

Quantitative Polymerase Chain Reaction

Total RNA was isolated using the RNeasy kit (Qiagen) and reverse transcripted into cDNA with a PrimeScriptTM RT Master Mix Kit (Takara). cDNA was amplified through 40 cycles. Quantitative reverse-transcription polymerase chain reaction was carried out with appropriate primers and iTaqTM Universal SYBR Green Supermix Kit (Bio-Rad) on a QuantStudio 7 Flex system (Life Technologies). All experiments were performed in triplicates. The final results were normalized by endogenous Glyceraldehyde 3-phosphate dehydrogenase (GAPDH) levels. The primers used in this study are shown in Table S2.

RNA Sequencing and Data Analysis

Total RNAs were isolated using an RNeasy kit (Qiagen). The RNA sequencing libraries were prepared by the TruSeq Stranded mRNA Library Prep kit (Illumina) and sequenced on HiSeq X-Ten sequencers with a paired-end 150 reads setting. Sequencing reads were aligned to human genome(hg19) using STAR version 2.6.1a. Transcripts per 1 million reads values were calculated using RSEM tools version 1.3.0. Differential gene expression was determined using DESeq2 version 1.20.0 with $\log_2$ fold change of > 1 and false discovery rate value of <0.05. The RNA sequencing data are from 2 biological samples. Gene ontology biological process analysis was conducted using the clusterprofiler R package version 3.6.1 (R Foundation for Statistical Computing) with a P value threshold of 0.01 and a q value threshold of 0.05. Gene interaction networks were plotted by the Search Tool for Retrieving Interacting Genes/Proteins database version 11.0.

Ligand-Receptor Interaction Network Analysis

Limbal stem/progenitor cell and LSSC gene expression values from the transcripts per 1 million reads list were filtrated by a threshold of >50. Mapping database from the work of Ramilowski et al[18] was used to analysis the ligand-receptor interaction network. The database includes the gene list from the Human Plasma Membrane Receptome, Ligand-Receptor Partners, the Human Protein Reference Database, the International Union of Basic and Clinical Pharmacology, and the Search Tool for Retrieving Interacting Genes/Proteins.

Immunofluorescence Staining

Cells were fixed overnight in 4% paraformaldehyde at 4 °C. Cells samples or slides were blocked in phosphate-buffered saline with 3% BSA and 0.3% Triton X-100, followed by primary antibodies incubating overnight at 4 °C. After washing with phosphate-buffered saline 3 times, cells were incubated with appropriate secondary antibodies for 2 hours at room temperature. Cell nuclei were sequentially counterstained with Hoechst 33342 (Invitrogen). Tissue samples or CEC sheet membranes were fixed in 10% neutral buffered formalin solution for 30 minutes at room temperature and were then embedded in paraffin and sectioned to 5-µm slides. After deparaffinization, slides were stained following the same protocol described above. Samples were imaged with a confocal laser scanning microscope (LSM 800; Zeiss). The antibodies used in this study are shown in Table S3.

Rabbit Limbal Stem Cell Deficiency Model and Cell Transplantation

All animal studies were conducted following the Association for Research in Vision and Ophthalmology Statement on the Use of Animals in Ophthalmic and Vision Research, and approvals were obtained by the Animal Care and Use Committee of Zhongshan Ophthalmic Center. The investigator who performed transplantation was masked to whether the LSSCs were used. Other investigators carried out assessment of the effect about corneal regeneration and were masked to the group information of the rabbits. All animals were grafted with allogeneic cells (LSC or LSC plus LSSC) in this study.

The LSCD model was created as previously reported.[19] Briefly, male New Zealand white rabbits (2−3 kg) were anesthetized with 2.5 mg/ml xylazine hydrochloride and 37.5 mg/ml ketamine hydrochloride. Surgery was performed in left eye of each animal model, and the right eye was used as a blank control. For topical anesthesia, 0.5% proparacaine was dropped into the eyes before the surgery. The entire limbal and corneal epithelium was removed with a blade to create a lamellar keratectomy from 2 mm outside the limbus at a depth of approximately 150 µm.

Cell Transplantation in Limbal Stem Cell Deficiency Model. Rabbits were randomly assigned into 3 groups. In the LSC group, immediately after the LSCD model was created, 150 µl collagen I (Gibco; 2 mg/mL; ph, 6.5−7.5) were added onto the denuded stroma (drop by drop with a 200-µl micropipette), and then we waited for 2 minutes. Next, an LSC sheet ($\Phi \approx 20$ mm) was added on the surface, and a human amniotic membrane (HAM) was then covered and secured by 10-0 nylon monofilament sutures (Alcon). In the LSC plus LSSC group, the LSSCs (1×10^6 cells) were mixed in 150 µL collagen I and seeded onto the exposed stromal bed. All other steps were the same as above. In the LSCD group, the denuded stroma was covered by 150 µL collagen I without cells and secured with HAM. Sutures and HAMs were removed at 7 days after surgery. TobraDex eyedrops (Alcon) were applied to all rabbit eyes after the surgery, administered as follows: 3 times daily for first 2 weeks, twice daily for the following 4 weeks, then once daily for 4 weeks, and finally once every other day for 2 weeks, gradually reduced and stopped within 3 months.

Cell Transplantation in the Post−Limbal Stem Cell Deficiency Model. Six to 9 weeks after the LSCD model was created, rabbits were randomly divided into 3 groups—a control group, LSC group, and LSC plus LSSC group—with no significant differences in corneal opacity or neovascularization among groups. After removal of the fibrovascular tissue over the corneal surface, cell transplantation was performed as previously mentioned. In the control group, HAM was secured after the collagen I treatment.

Evaluation of Corneal Regeneration

Corneal epithelial defects, neovascularization, and opacity were photographed with slit-lamp biomicroscopy and assessed every 3 weeks by 3 different investigators. To assess the epithelial defect, fluorescein-stained regions of the corneal surface were measured using ImageJ (National Institutes of Health). Neovascularization was scored as follows: 0 = none; 1 = area less than or equal to one-quarter, 2 = one-quarter less than area less than or equal to one-half, 3 = one-half less than area less than or equal to three-quarters, and 4 = area greater than three quarters.[20] Corneal opacity was scored as following scale: 0 = none, 1 = mild, 2 = moderate, 3 = severe, pupil seen faintly, and 4 = severe, pupil not visible.[21] Success was defined as the sum of the neovascularization and opacity scores of <5 at week 24 after transplantation. Otherwise, the treatment was considered a failure.

Statistical Analysis

The data are presented as mean ± standard error of the mean, unless otherwise noted. For qualitative variables, the differences between groups were analyzed by the Kruskal-Wallis test. The Friedman test was used to compare values over time. For quantitative data, a statistical 2-way analysis of variance and upaired

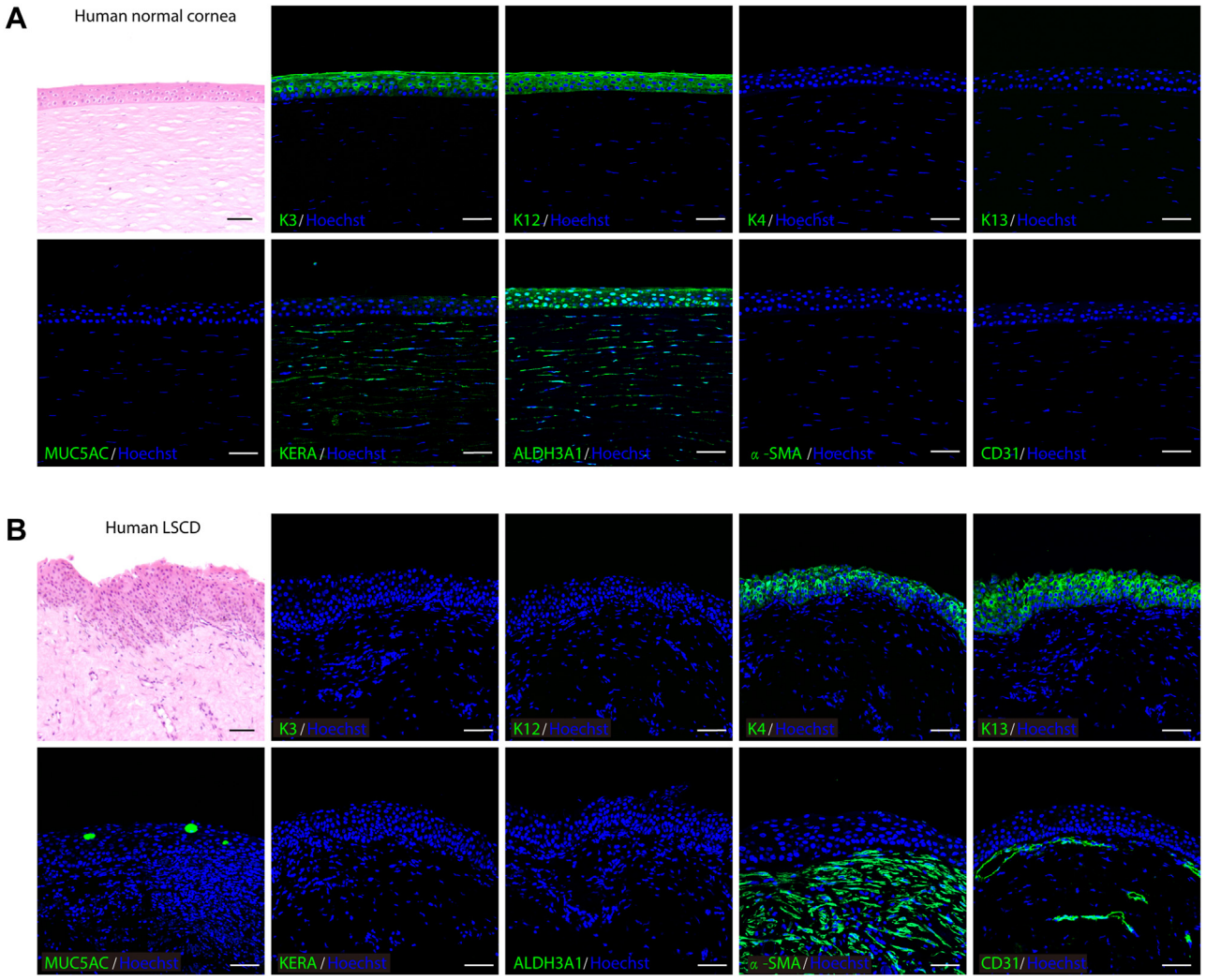

Figure 1. Photomicrographs showing normal and pathologic changes of corneal tissues. **A**, **B**, Hematoxylin–eosin staining (top left panel) and immunofluorescence staining (all others) of keratins, MUC5AC, KERA, ALDH3A1, alpha smooth muscle actin (α-SMA), and CD31 in (**A**) normal human corneal tissue and (**B**) corneal tissue from a patient with limbal stem cell deficiency (LSCD). Scale bars, 50 μm.

Student *t* test were performed for statistical analysis. The log-rank (Mantel-Cox) test was used to analyze survival rate.

Results

Pathologic Changes in Corneal Epithelium and Stroma Tissues of Patients with Limbal Stem Cell Deficiency

Normal human corneas consist of an orderly arrangement of epithelial cells and collagen fibers,[22] whereas abnormal tissue structures with neovascularization are observed in patients with LSCD.[23] Replacing cornea-specific keratin K3/K12 with conjunctiva-specific K4/K13 and the goblet cell marker MUC5AC seemed to cause LSC dysfunction and migration of the conjunctival epithelium to the corneal surface (conjunctivalization). In addition, the corneal stroma of patients with LSCD did not express keratocyte-specific markers (KERA and ALDH3A1), but showed positive results for alpha smooth muscle actin (α-SMA) and CD31 (Fig 1A, B). These pathologic changes indicated the loss of functional keratocytes and the presence of fibroblasts and blood vessels, which led to stromal opacity and vision impairment. Based on the homeostatic disruption of both the corneal epithelium and stromal tissues in patients with LSCD, we aimed to reconstruct their corneas by cotransplanting LSCs and LSSCs.

Ex Vivo Expansion and Differentiation of Limbal Stem/Progenitor Cells and Limbal Stromal Stem/Progenitor Cells under Serum-Free Conditions

Using undefined animal products not only raises safety concerns when manufacturing cells for clinical applications, but also introduces barriers to the investigation of cellular mechanisms.[24] Serum-free and feeder-free culture conditions were established to expand human LSCs and LSSCs. The cultured LSCs were characterized as positive for PAX6 and p63 expression (Fig 2A). At high population densities, a

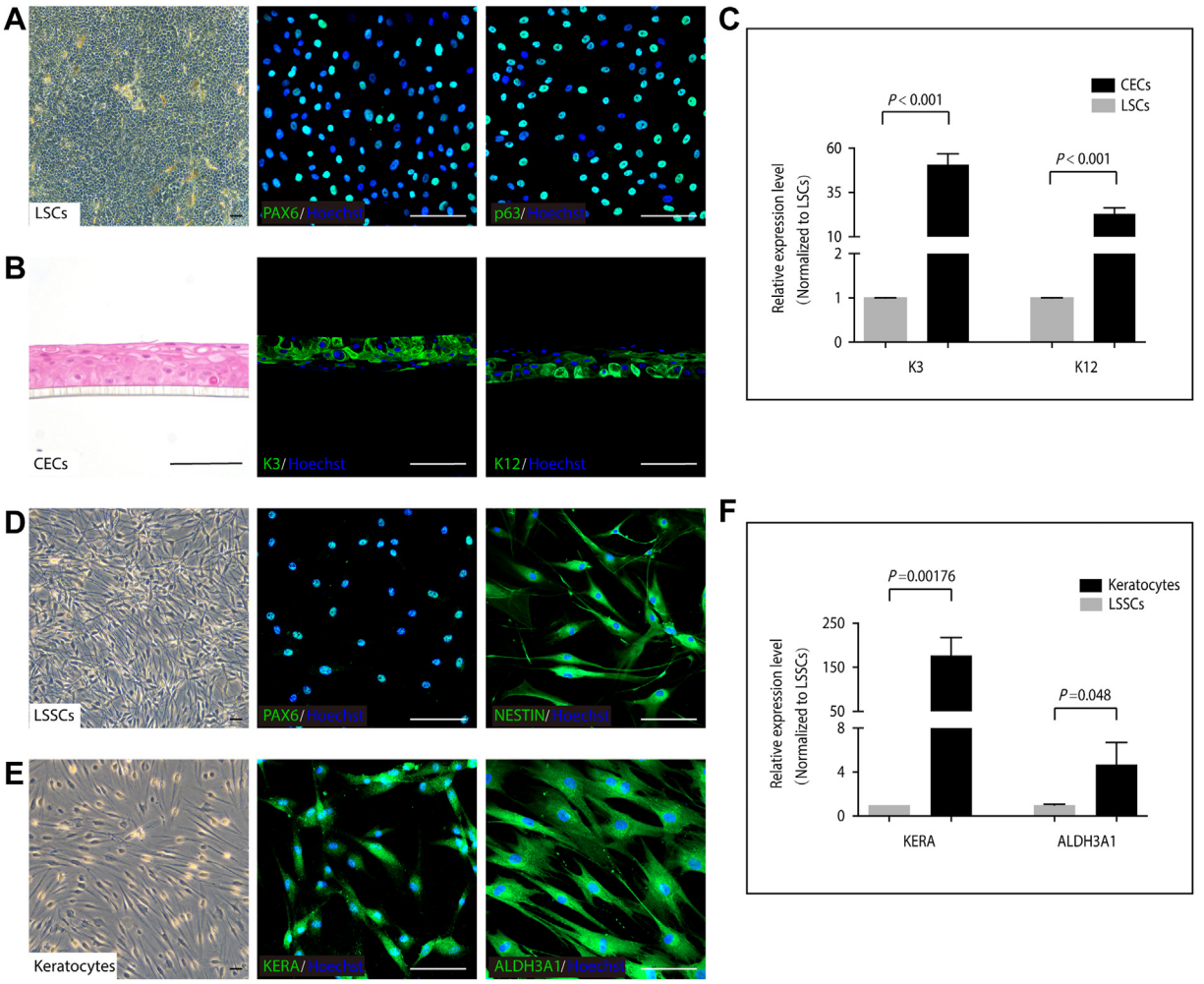

Figure 2. Characterization of human limbal stem/progenitor cells (LSCs), Limbal stromal stem/progenitor cells (LSSCs), and their differentiated cells. **A**, PAX6 and p63 immunofluorescence staining in cultured LSCs. **B**, **C**, Immunofluorescence staining (**B**) and quantitative polymerase chain reaction (qPCR) analysis (**C**) of K3 and K12 in air-lifting differentiated corneal epithelial cells (CECs). **D**, PAX6 and NESTIN immunofluorescence staining in cultured LSSCs. **E**, **F**, Immunofluorescence staining (**E**) and qPCR analysis (**F**) of KERA and ALDH3A1 in differentiated keratocytes. *P* values in (**C**) and (**F**) were determined by unpaired Student *t* test (n = 3). Data are presented as mean ± standard deviation. Scale bars, 100 μm.

monolayer of tightly connected LSCs (LSCs sheet) could be peeled off from the culture dish (Fig 3A). When cultivated on an air−liquid interface, LSCs generated a multilayered epithelium in 6 to 12 days. The epithelium expressed high levels of the corneal epithelium-specific markers K3 and K12, which indicated that the LSCs effectively differentiated into CECs (Fig 2B, C). Limbal stromal stem/progenitor cells exhibited dendritic morphologic features as well as PAX6 and NESTIN expression (Fig 2D). These cells further differentiated into keratocytes, as evidenced by positive staining for *KERA* and *ALDH3A1* (Fig 2E). These two signature genes were significantly upregulated in differentiated cells compared with those in LSSCs (Fig 2F).

Cotransplantation of Limbal Stem/Progenitor Cells and Limbal Stromal Stem/Progenitor Cells in a Rabbit Model of Limbal Stem Cell Deficiency

The therapeutic effect of cotransplanting LSCs and LSSCs was evaluated using a rabbit model of LSCD with induced corneal opacity and neovascularization (Fig 3A, B). Rabbit LSCs and LSSCs were cultured and characterized. The LSCs exhibited K19, PAX6, and p63 expression, and the LSSCs exhibited PAX6, ABCG2, and NESTIN expression (Fig S1A, B). The LSCD model was created by lamellar keratectomy with an average depth of approximately 150 μm (Fig 3C, D). In the LSC group, the exposed stromal bed was receiving collagen I and LSCs sheet at the time of wounding. In the LSC plus LSSC group, LSSCs were mixed with collagen I and seeded onto the stromal bed, and then covered with an LSCs sheet (Fig 3A). The degree of corneal opacity and neovascularization was calculated based on a scoring system (Fig 3E) every 3 weeks. Success was defined as a sum of the 2 scores of < 5 at week 24 after transplantation. Otherwise, the treatment was considered a failure.

Typical signs of LSCD, such as corneal neovascularization and opacity, began to appear in the LSCD group at 3 weeks (Fig 3B, Fig S2). Notably, both LSC

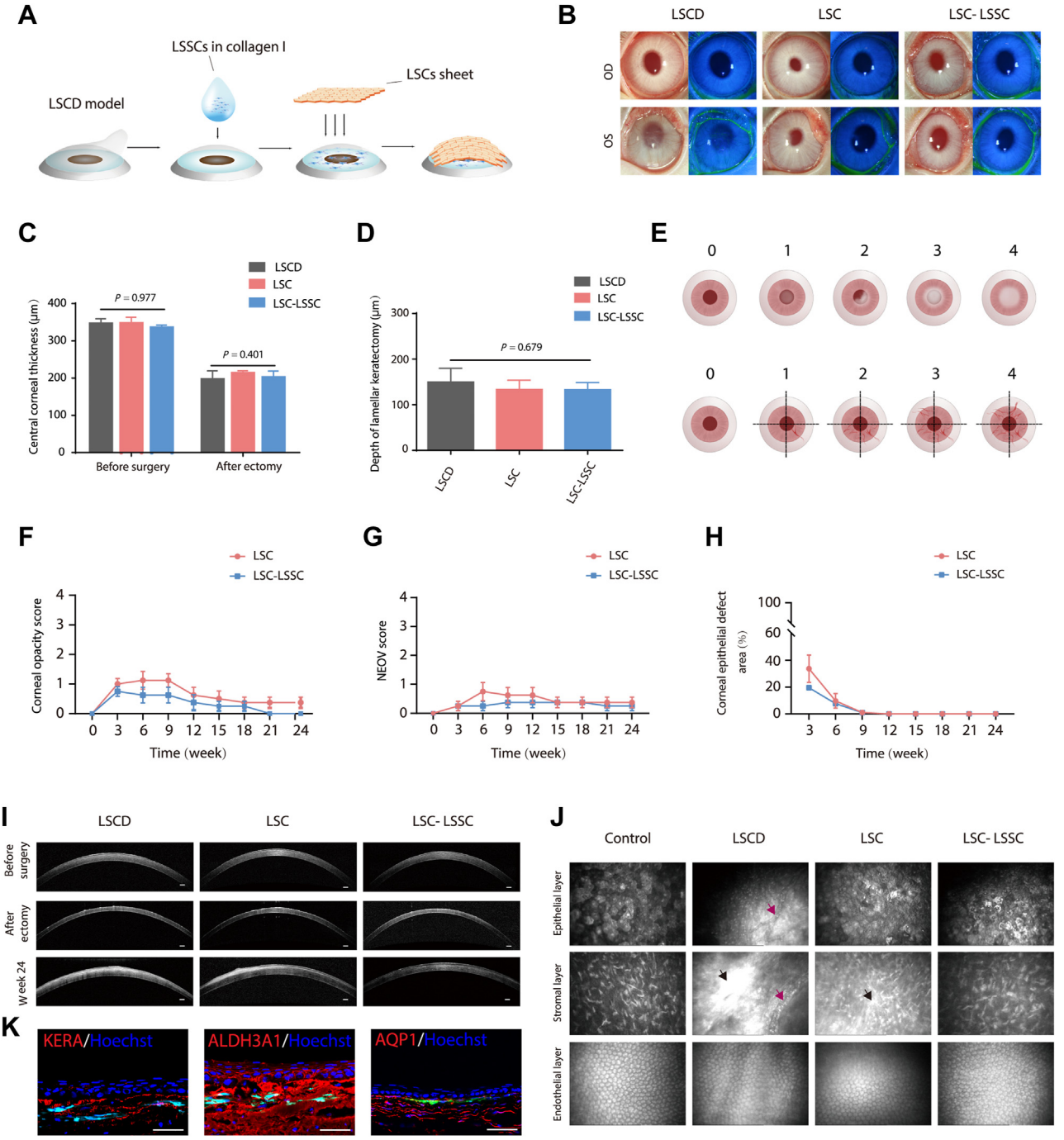

Figure 3. Cell transplantation and corneal regeneration in rabbit limbal stem cell deficiency (LSCD) model. **A**, Schematic diagram of cotransplantation of limbal stem/progenitor cells (LSCs) and limbal stromal stem/progenitor cells (LSSCs). **B**, Representative images of rabbit corneas 24 weeks after surgery (left panel, white light micrograph; right panel, fluorescein dye staining of corneal epithelium surface; right eye [OD] as control and left eye [OS] as surgical eye). **C**, Graph showing central corneal thickness of each group in the LSCD model before and after keratectomy based on the OCT results. No significant difference was found among groups (control group, n = 3; LSC group, n = 8; LSC-LSSC group, n = 8). **D**, Graph showing that the average depth of keratectomy was approximately 150 μm. **E**, Scoring system of corneal opacity and neovascularization. Corneal opacity scale appears in the upper panel: 0, none; 1, mild; 2, moderate; 3, severe, pupil seen faintly; and 4, severe, pupil not visible. Neovascularization scale appears in the lower panel: 0, none; 1, area $\leq$ 1/4; 2, 1/4 < area $\leq$ 1/2; 3, 1/2 < area $\leq$ 3/4; and 4, area > 3/4. **F**, **G**, Graphs showing statistical analysis of the corneal opacity (**F**) and neovascularization (NEOV) (**G**) (Kruskal-Wallis test, n = 8). **H**, Graph showing statistical analysis of corneal epithelial defect area (unpaired Student *t* test, n = 8). **I**, **J**, Representative (**I**) OCT and (**J**) in vivo confocal microscopic images of rabbit corneas 24 weeks after surgery (black arrow, dense scar-like hyper reflective deposits; purple arrow, blood vessels). Scale bars, 200 μm. **K**, Immunofluorescence staining of corneal stroma-specific markers (KERA, ALDH3A1, and AQP1) in rabbit LSCD model corneas treated with LSCs and ZsGreen-labeled LSSCs (3 weeks after transplantation). Scale bars, 50 μm.

transplantation and LSC plus LSSC cotransplantation effectively repaired the corneal surface and maintained corneal clarity for > 24 weeks (Fig 3B, Figs S3 and S4). These 2 transplantation strategies showed no significant differences in terms of the graft survival rate or epithelial repair (Fig 3F–H, Tables S4–S7). As expected, the regenerated corneal epithelium of both groups stained with positive results for K3/12 and with negative results for the conjunctival epithelial markers K4/K13 and MUC5AC (Fig 4). Blood vessels could be found only in the LSCD group without cell treatment (Fig 3B, J). However, bright stromal regions and irregular corneal structures were observed using OCT in the LSC group (in 3 of the 8 rabbits; Fig S5), but not in the LSC plus LSSC group (Fig 3I, Fig S6). This is consistent with the dense, scar-like, hyperreflective deposits found in this group (Fig 3J), indicating that corneal fibrosis occurred in the LSC group. Immunofluorescence staining further confirmed the presence of the fibrotic marker α-SMA and the partial absences of KERA and ALDH3A1 expression in the stromal regions of the LSC group. In comparison, abundant KERA and ALDH3A1 expression without detectable α-SMA expression was observed in the LSC plus LSSC group (Fig 4).

To assess the capability of the transplanted LSSCs for corneal regeneration, LSCs and ZsGreen-labeled LSSCs were applied to the wound bed for short-term tracking. These labeled cells were observed in the anterior stroma and showed positive results for KERA, ALDH3A1, and AQP1 at 3 weeks after transplantation (Fig 3K), demonstrating that the LSSCs differentiated into keratocytes during the wound-healing process. Collectively, these data indicated that the implanted LSSCs could prevent corneal scar formation and could regenerate the injured stroma, thus potentially improving vision in the LSCD model when cotransplanted with LSCs.

Enhanced Corneal Regeneration in a Post-Limbal Stem Cell Deficiency Model via Limbal Stem/Progenitor Cell and Limbal Stromal Stem/Progenitor Cell Cotransplantation

Considering that patients with LSCD usually exhibit corneal vascularization and opacity before surgical treatment, 2 transplant strategies were also tested using a rabbit model in which transplantation was performed after clinical signs were induced in an LSCD model (pLSCD) 6 to 9 weeks after LSCD surgery. The pLSCD rabbits were randomly divided into 3 groups (control group, LSC group, and the LSC plus LSSC group). No significant difference was detected in the total score of neovascularization or corneal opacity among the groups (Fig 5A, Table S8). The fibrovascular tissue was removed, and the cells were transplanted onto the denuded cornea, as previously described.

At 24 weeks after surgery, we observed improved corneal clarity and reduced neovascularization in both the LSC and LSC plus LSSC groups, whereas no improvement could be found in the control group (Fig 5B, C, Figs S7 and S8). Surprisingly, cotransplantation with LSCs and LSSCs produced significantly better outcomes in terms of the invasion of blood vessels (Fig 5D, Figs S7 and S8, Table S9) and the regularity of corneal structure (Figs 5E and 6A, Figs S9 and S10, Table S10). The graft survival rate in the LSC plus LSSC group was 87.5%, which was significantly higher than that in the LSC group (37.5%; $P < 0.05$; Fig 5F, Table S11). Treatment failure in the 2 groups occurred between 6 and 15 weeks after surgery (survival rate of the LSC group was 62.6% at 6 weeks and 37.5% at 9 weeks; survival rate of the LSC plus LSSC group was 87.5% at 15 weeks). Moreover, healing of the corneal epithelial defects in the LSC plus LSSC group accelerated significantly at 3 weeks after surgery ($P < 0.05$; Fig 5G, Table S12).

In most cases, OCT and in vivo confocal microscopy images revealed that the corneal stroma in the LSC plus LSSC group featured a regular corneal structure with ordered arrangement of cells, whereas blood vessels and stromal scars were observed in the LSC group (Fig 6A, B, Figs S9 and S10). As expected, a large area of α-SMA–positive cells was found in the LSC group during whole-mount corneal staining, whereas only dispersed staining was observed in the LSC plus LSSC group (Fig 6C). More importantly, immunostaining of the successfully reconstructed corneas (total score, <5) in the LSC plus LSSC group at 24 weeks after surgery revealed that $K14^+/p63^+$ cells at the limbus were adjacent to $K3^+/12^+$ cells at the peripheral cornea, similar to the structure of normal rabbit corneas (Fig 6D). These data suggest that cotransplanting LSCs and LSSCs regenerated a functional limbus, indicating the potential of this approach for sustaining long-term corneal transparency.

Extracellular Factors of Stromal Cells in Corneal Regeneration

Given the advantage of LSC plus LSSC cotransplantation in pLSCD treatment, we further investigated the potential role of LSSCs in corneal recovery. The RNA sequencing data were generated from cultured epithelial and stromal cells (Fig S11A). Gene ontology analysis showed that genes upregulated in LSSCs were preferentially associated with extracellular structure and matrix organization, sulfur compound and glycosaminoglycan biosynthetic process, and eye development. Interestingly, the enriched genes in LSSCs were also linked to axonogenesis and neuron-projection guidance, suggesting a potential contribution to nerve regrowth (Fig S11B).

To explore possible LSSC-to-LSC communication after transplantation, we selected genes encoding secreted proteins of LSSCs and the corresponding receptors of LSCs to analyze ligand–receptor pair interactions. Among these pairs, LSSC-secreted collagens (e.g., COL1 and COL14A1) and laminins potentially bind to integrins produced by LSCs, thereby supporting epithelial cell adhesion and migration during the wound-healing process.[25] Of note, HGF-Met and collagen–discoidin domain receptor 1 interactions are known to promote epithelial cell proliferation (Fig S11C, D).[26,27] In addition, dickkopf-related protein 2, known as a crucial regulator of the corneal homeostasis,[28] and VEGF receptor-1, an essential factor for preserving

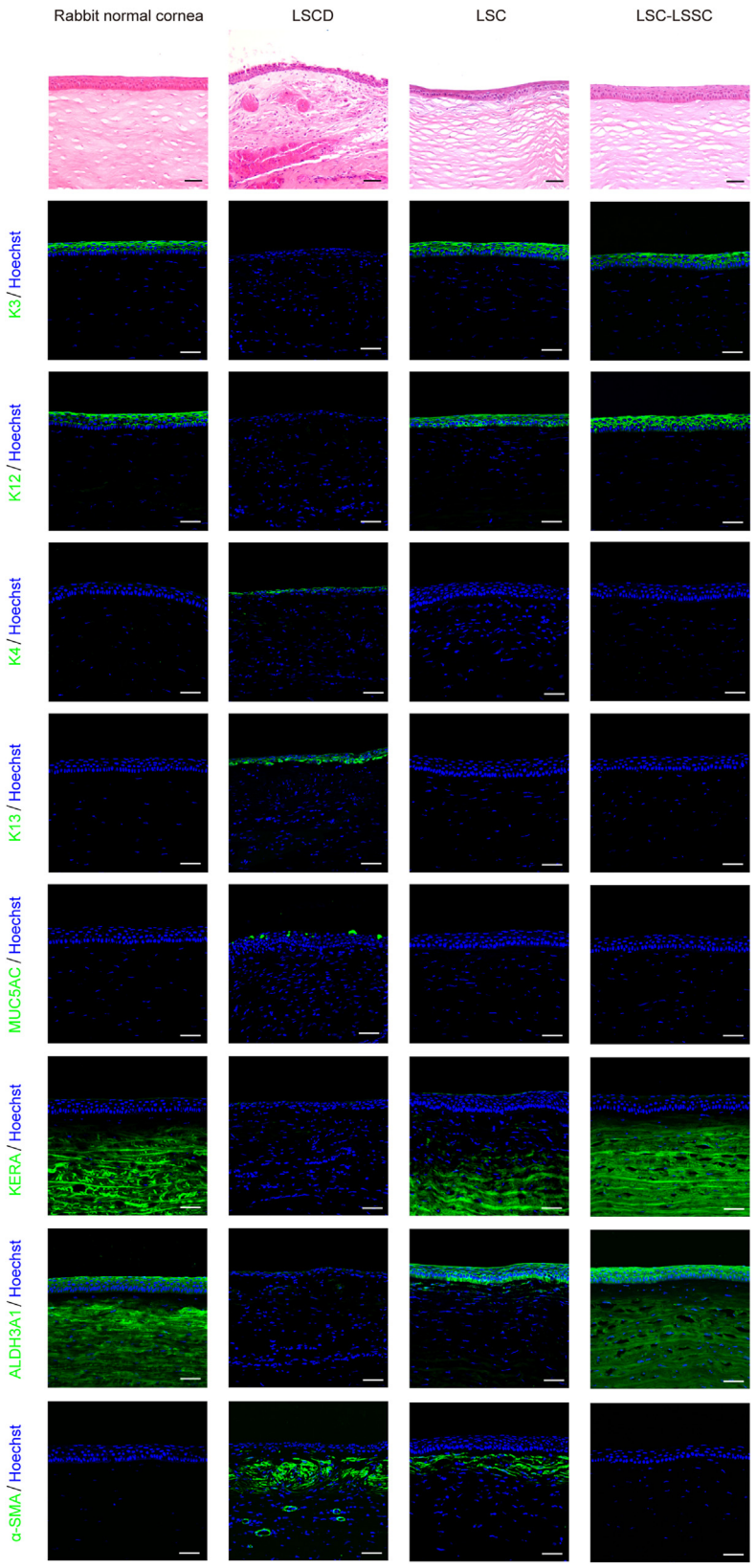

Figure 4. Photomicrographs showing characterization of the regenerated cornea in the rabbit limbal stem cell deficiency (LSCD) model. Representative images of hematoxylin–eosin staining (top row) and immunostaining images (all others) of epithelial markers of cornea (K3 and K12) and conjunctiva (K4, K13, and MUC5AC), corneal stroma-specific markers (KERA and ALDH3A1), and fibroblast marker alpha smooth muscle actin (α-SMA) in the rabbit LSCD model corneas at 24 weeks after transplantation. Scale bars, 50 μm. LSC = limbal stem/progenitor cells; LSSC = limbal stromal stem/progenitor cell.

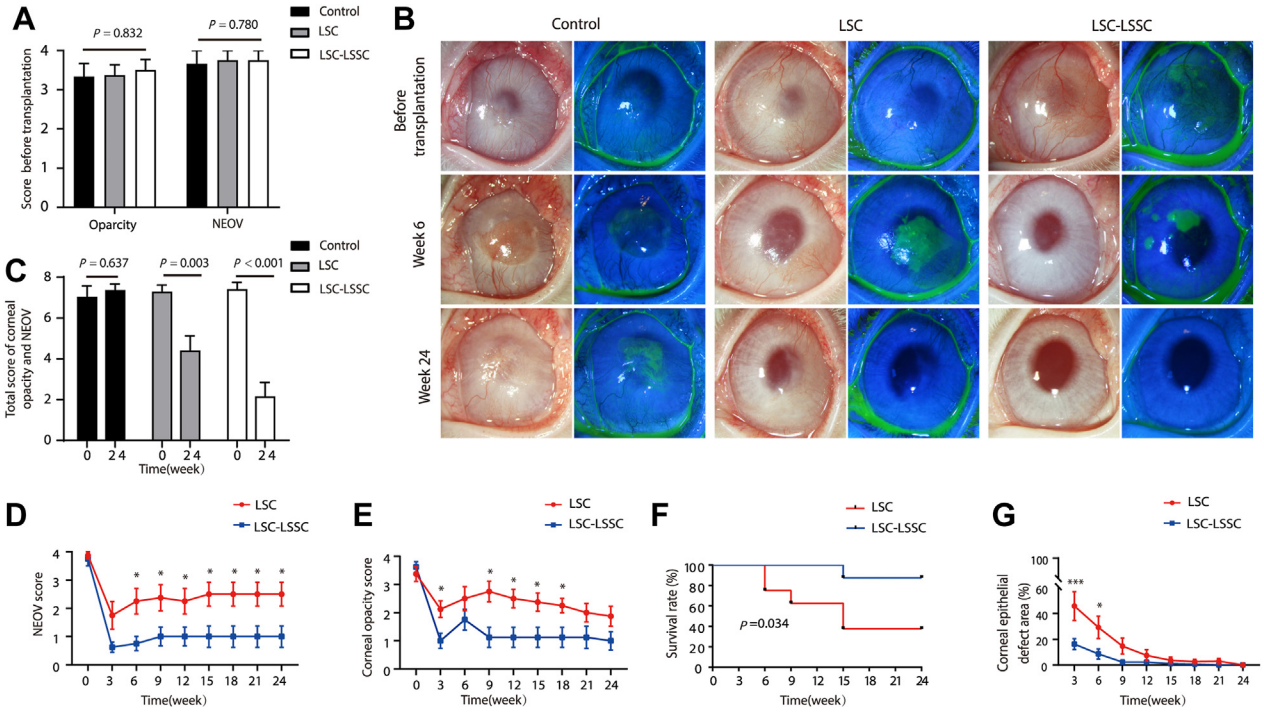

Figure 5. Cell transplantation and ocular surface evaluation in a rabbit model in which transplantation was performed after clinical signs were induced in a limbal stem cell deficiency (LSCD) model. **A**, Graph showing scores of corneal opacity and neovascularization (NEOV) in the control group (n = 3), limbal stem/progenitor cell (LSC) group (n = 8), and LSC plus limbal stromal stem/progenitor cell (LSSC) group (n = 8) before transplantation (Kruskal-Wallis test). **B**, Representative images of post-LSCD (pLSCD) rabbit models (left panel, white light micrograph; right panel, fluorescein dye staining of corneal epithelium surface). **C**, Graph showing total score of corneal opacity and NEOV in the control group (n = 3), LSC group (n = 8), and LSC-LSSC group (n = 8; Kruskal-Wallis test). **D**, **E**, Graphs showing statistical analyses of the (**D**) NEOV and (**E**) corneal opacity scores between the LSC and LSC-LSSC groups (Kruskal-Wallis test; n = 8). **F**, Graph showing total score of corneal opacity and NEOV assessed at week 24. For failure sample (the sum of corneal opacity and NEOV scores of ≥5 at week 24), the time point of failure was set in the earliest week when the score was ≥5 and without any improvement until 24 weeks. Kaplan-Meier analysis was used to estimate the grafted cells survival (success rate attained in 87.5% of LSC-LSSC group and 37.5% of LSC group 24 weeks after transplantation; log-rank [Mantel-Cox] test; n = 8). **G**, Graph showing quantification of corneal epithelial defect area percentage in the LSC and LSC-LSSC groups (unpaired Student *t* test; n = 8). *P* values are presented in Supplemental Tables S9, S10, and S12. $^{*}P < 0.05$; $^{**}P < 0.01$; $^{***}P < 0.001$.

corneal avascularity,[29] were found to be expressed in LSSCs, but not in fibroblasts (Fig S11D). This suggests that LSSCs serve diverse roles in communication with epithelial cells and regulation of the local niche during corneal regeneration.

Considering that the transplanted LSSCs were detected to differentiate into keratocytes within 3 weeks (Fig 3K), upregulated genes in keratocytes were inferred based on associated gene ontology biological process terms using the Search Tool for Retrieving Interacting Genes/Proteins database. Network connectivity analysis identified a series of genes that were highly expressed in keratocytes and their possible functions (Fig 7A, B). These genes included *HGF* (a notable gene for re-epithelization),[30] *KERA*, *LUM*, *DCN*, *OGN*, and collagens, producing components of keratan sulfate proteoglycans or corneal stroma.[31] Moreover, anti-inflammatory factors (apolipoprotein D and apolipoprotein E), anti-angiogenic factors (ADAM Metallopeptidase with Thrombospondin Type 1 Motif 9 and semaphorin 3A), and axon growth-related factors (brain-derived neurotrophic factor and neuron-glial related cell adhesion molecule) were also found in this network (Fig 7A, B).

We further confirmed the expression of several signature genes in cultured cells and corneal tissues. Positive staining for COL1, semaphorin 3A, apolipoprotein D, HGF, and neuron-glial related cell adhesion molecule was observed in keratocytes, but not in fibroblasts (Fig 7C). These genes were also detected in normal human corneas, but were absent in the corneal tissues of patients with LSCD (Fig 7D). Consistent with these findings, the above genes were expressed by differentiated LSSCs in the anterior corneal stroma 3 weeks after cotransplantation of LSCs and ZsGreen-labeled LSSCs (Fig 7E), and these genes exhibited a sustained expression pattern in the corneal stroma of the LSC plus LSSC group (total score, <5, pLSCD model; Fig 7E). Together, these data suggest that keratocytes play multiple roles in the corneal-regeneration niche, including the inhibition of inflammation and angiogenesis and promotion of epithelial repair and extracellular matrix assembly.

Discussion

Limbal stem cell deficiency leads to severe destruction of the ocular surface and loss of vision.[32] In previous decades, treatments for this disease have mainly focused on supplementation with LSCs and reconstruction of the

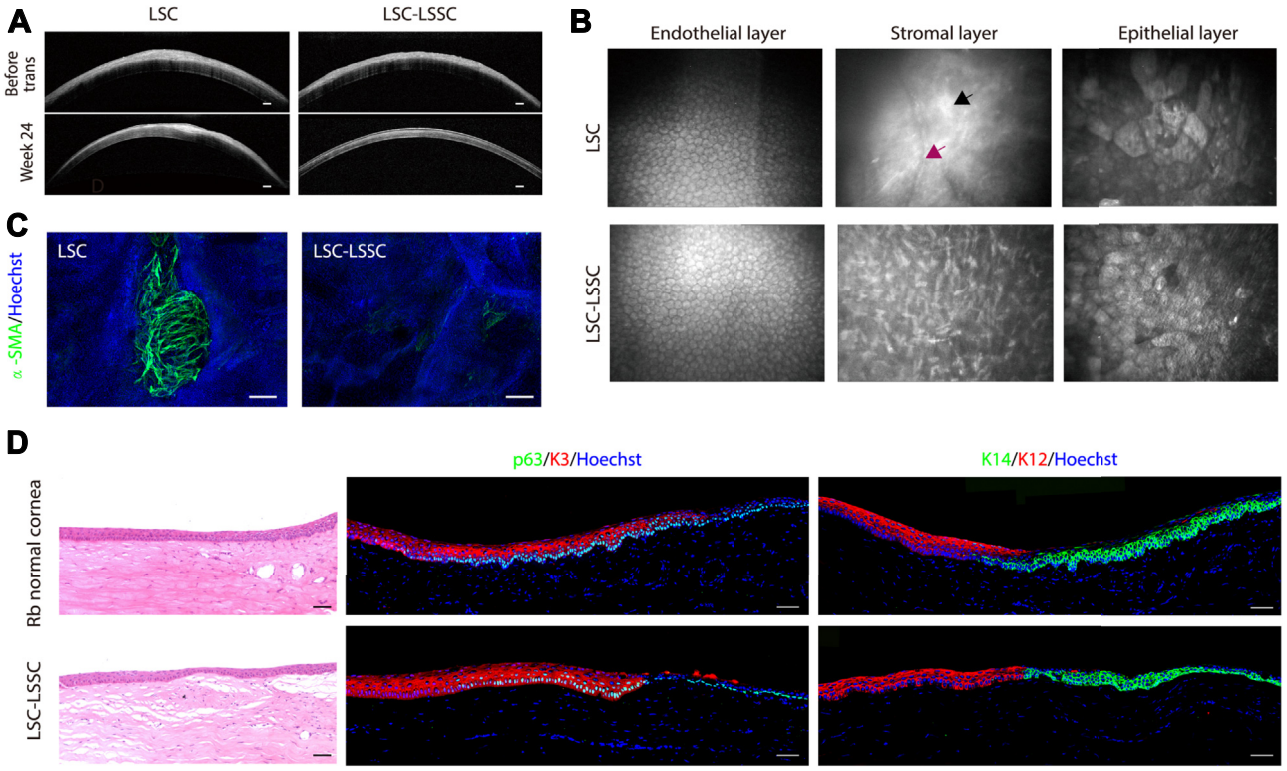

Figure 6. Cell transplantation and regeneration of corneal stroma and limbus in a rabbit model in which transplantation was performed after clinical signs were induced in a limbal stem cell deficiency model. **A**, **B**, Representative (**A**) OCT and (**B**) in vivo confocal microscopic images showing rabbit corneas at 24 weeks after transplantation (black arrow, dense scar-like hyperreflective deposits; purple arrow, blood vessels). Scale bars, 200 μm. **C**, Whole-mount immunostaining of alpha smooth muscle actin (α-SMA) in rabbit corneas of limbal stem/progenitor cell (LSC) and LSC plus limbal stromal stem/progenitor cell (LSSC) groups. Scale bars, 200 μm. **D**, Photomicrographs showing representative images of hematoxylin–eosin staining (left panels) and immunofluorescence staining (right panels) of limbal- and corneal-specific markers in rabbit corneal limbus 24 weeks after transplantation. Scale bars, 50 μm.

corneal epithelium.[33] However, persistent damage in the stroma, such as fibrosis and structural disorganization, cannot be completely repaired by LSC transplantation. Herein, we introduced cotransplantation of LSCs and LSSCs as a new strategy for LSCD treatment and found that this approach resulted in a significantly improved therapeutic effect.

The surgical and alkali burn LSCD models are widely used for studies of corneal regeneration.[34] However, the burning scope and depth in the alkali burn model are uncontrollable, which will lead to the residue of LSCs and the inaccurate evaluation of the function of the transplanted cells. Thus, the surgical model was used to ensure the complete removal of LSCs and the corneal epithelium. Of note, LSCs enabled successful reconstruction of injured corneas when transplantation was performed immediately after removal of the limbus and corneal surface, but LSCs showed limited efficacy when hallmark features of LSCD were induced in the pLSCD model. This result is consistent with a previous report showing that normal vision was restored only in patients with LSCD with undamaged corneal stroma, and keratoplasty was required to improve visual acuity after LSC grafting.[33] Therefore, homeostasis of the corneal stroma is crucial for LSC-mediated epithelial regeneration and the ultimate quality of visual function. Intervention in the acute phase of corneal injury is desirable to avoid severe stromal disorder, which may also contribute to the re-epithelization of residual LSCs.

Scar-free treatment is the ultimate goal of corneal regeneration. Multiple studies revealed that the inflammatory response leads to the formation of corneal stromal fibrosis in the wound-healing process.[35] Mesenchymal stem cells (MSCs) have been used to restore corneal transparency after ocular injury.[36] Although no evidence exists that MSCs can differentiate into corneal stromal cells, it is believed that the secretome of MSCs exert immunomodulatory functions.[37] Hepatocyte growth factor secreted by MSCs in an inflammatory environment has been shown to suppress the conversion of stromal cells into fibroblasts after corneal injury.[30] Hepatocyte growth factor also was found to be expressed in both LSSCs and keratocytes in this study. It is possible that LSSCs and MSCs share similar gene expression profiles and cellular functions. The comparison between the 2 lineages would find more protective factors in decreasing the risk of corneal scarring. Recently, multilineage-differentiating stress-enduring cells isolated from lipoaspirates were differentiated into corneal stromal cells with keratocyte markers.[38] Implantation of these multilineage-differentiating

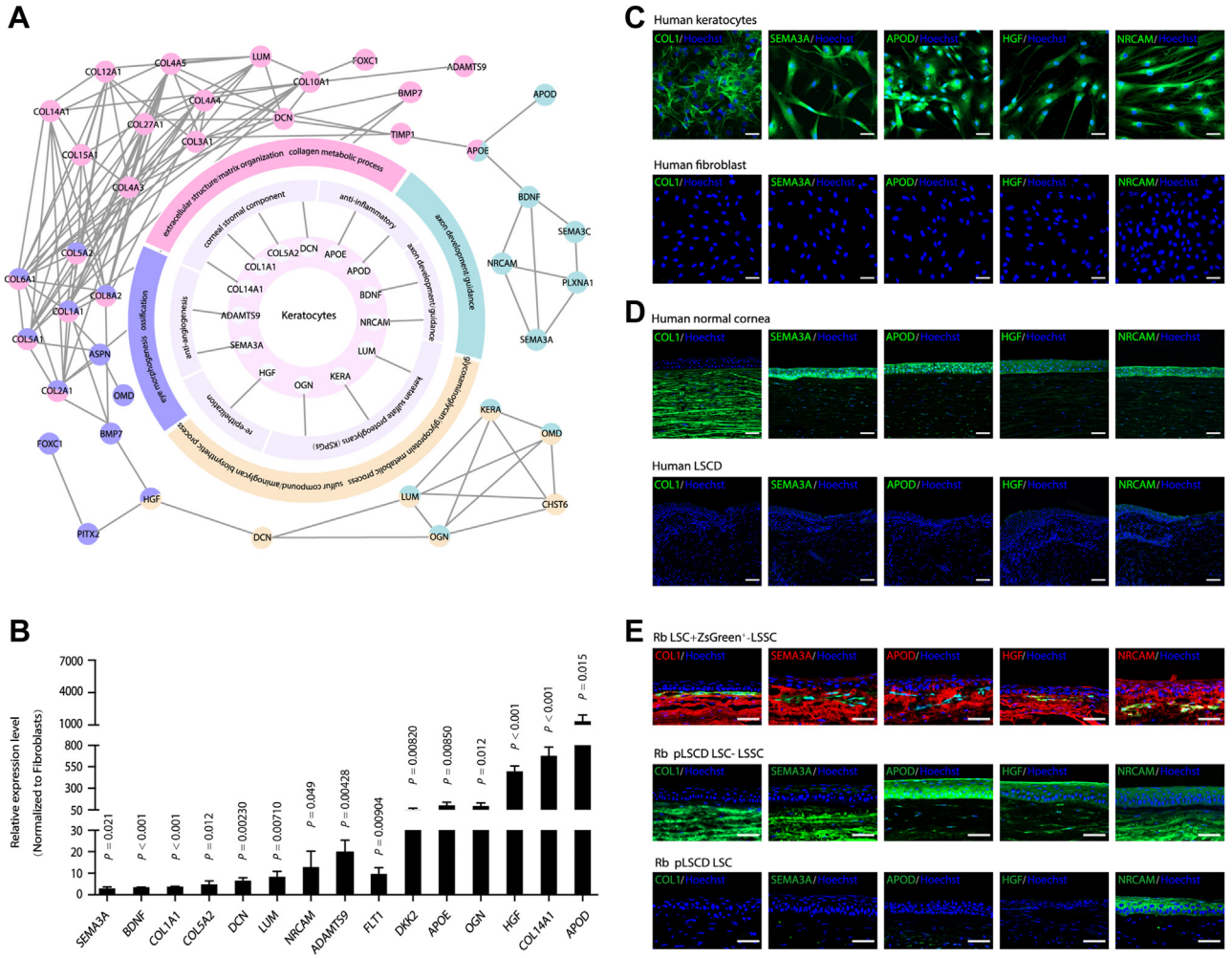

Figure 7. Secretory factors of keratocytes in corneal regeneration. **A**, Diagram showing the network of the upregulated genes of keratocytes versus fibroblasts. The outer cycle shows the selected gene ontology (GO) terms. The middle cycle represents gene functions in corneal regeneration. The inner cycle shows genes corresponding to the middle cycle. The outer network represents the interaction network between genes of GO terms. Genes and corresponding events are in the same color. **B**, Quantitative polymerase chain reaction showing results showing selected gene expression in keratocytes (unpaired Student *t* test; n = 3). Data are presented as mean ± standard deviation. **C**, Expression of the selected genes in cultured human keratocytes (top row) and human fibroblast (bottom row). **D**, Immunofluorescence-stained images showing selected genes' expressions in human normal (top row) and limbal stem cell deficiency (LSCD) (bottom row) corneas. **E**, Representative immunofluorescence staining images of selected genes' expressions in rabbit corneas after transplantation: LSCD model with limbal stem/progenitor cells (LSCs) and ZsGreen-labeled limbal stromal stem/progenitor cells (LSSCs; 3 weeks after surgery; top row), rabbit model in which transplantation was performed after clinical signs were induced in an LSCD model (pLSCD) with LSCs and LSSCs (24 weeks after surgery; middle row), and pLSCD model with LSCs (24 weeks after surgery; bottom row). Scale bars, 50 μm. ADAMTS9 = ADAM Metallopeptidase with Thrombospondin Type 1 Motif 9; APOD = apolipoprotein D; APOE = apolipoprotein E; BDNF = brain-derived neurotrophic factor; DKK2 = dickkopf-related protein 2; FLT1 = VEGF receptor-1; HGF = hepatocyte growth factor; NRCAM = neuron-glial related cell adhesion molecule; SEMA3A = semaphorin 3A

stress-enduring–derived cells not only prevented scar formation, but also increased re-epithelization and nerve regrowth in a corneal wound model. Similarly, we observed higher nerve density in the LSC plus LSSC group than in the LSC group in the LSCD model, whereas almost no subbasal nerves were found in the pLSCD model (data not shown). We concluded that corneal nerve recovery may require more time or additional treatment because the niche had been severely disturbed during the waiting time for cell transplantation in pLSCD.

The local stromal environment is highly active during wound healing, including inflammatory reactions, fibroblast migration, and angiogenesis.[39] These responses could be a challenge to corneal regeneration because of its unique structure and avascular nature.[40] Previous studies pointed out that the corneal extracellular matrix and sulfated glycosaminoglycans are crucial for maintaining corneal transparency.[41] Based on our findings, a close correlation and similar gene expression pattern exist between LSSCs and keratocytes. Gene ontology analysis showed that these 2 cells share the same gene ontology terms, including extracellular structure and matrix organization and sulfur compound and glycosaminoglycan biosynthetic process. Moreover, COL1A1, COL14A1, and dickkopf-related

protein 2 are common factors secreted by both LSSCs and keratocytes. Thus, although the grafted ZsGreen-labeled LSSCs may have differentiated into keratocytes within 3 weeks after transplantation, we assume both LSSCs and the differentiated keratocytes hold great potential for corneal niche homeostasis in the early phase of corneal healing. Further studies are needed to uncover the specific role of LSSCs and keratocytes in the wound-healing process.

Cell−cell interaction is believed to make a critical contribution in cell proliferation and migration in epithelial wound healing.[42] The ligand−receptor pair interaction analysis revealed a deep communication between LSCs and LSSCs. Collagens (e.g., COL1A1 and COL14A1) and lamininns secreted by LSSCs probably bind to integrins expressed by LSCs. The collagen/laminin and integrin pairs were reported for sustaining epithelial cell adhesion and migration in tissue regeneration.[43] Additionally, HGF-MET and collagen-Discoidin domain receptor 1, the well-known pairs for promoting epithelial cell proliferation, were also found in this network.[26,27]

Although a set of candidate genes that may be involved in re-epithelization and antiscarring is listed, future studies should identify their molecular functions in models of corneal injury. In addition, multiomics analysis and lineage tracing experiments to investigate the dynamic changes and underlying mechanisms of corneal regeneration by LSC plus LSSC transplantation will be required.

In summary, our study provided serum-free culture conditions for LSCs and LSSCs, revealed the multiple functions of stromal cells in corneal niche remodeling, and demonstrated the advantage of cotransplantation of LSCs and LSSCs in LSCD treatment. Such strategies elucidate the importance of niche homoeostasis and improve the effect of stem cell-based therapies in regenerative medicine.

Footnotes and Disclosures

Originally received: December 21, 2021.
Final revision: March 20, 2022.
Accepted: March 21, 2022.
Available online: March 26, 2022. Manuscript no. XOPS-D-21-00246.

State Key Laboratory of Ophthalmology, Zhongshan Ophthalmic Center, Sun Yat-sen University, Guangzhou, China.

*The authors Liqiong Zhu, Wang Zhang, and Jin Zhu contributed equally as first authors.

Disclosure(s):

All authors have completed and submitted the ICMJE disclosures form.

The author(s) have no proprietary or commercial interest in any materials discussed in this article.

Supported by the Projects of International Cooperation and Exchanges, Natural Science Foundation of China (grant no.: 32061160364 [H.O.]); the National Natural Science Foundation of China (grant no.: 31771626 [H.O.]); and the China Postdoctoral Science Foundation (grant no.: 2021M693625 [L.Z.]).

HUMAN SUBJECTS: Human subjects were included in this study. All human corneal tissues from donor samples were obtained from the eye bank (Zhongshan Ophthalmic Center) with the approval of the Ethics Committee of Zhongshan Ophthalmic Center of Sun Yat-sen University. All research adhered to the tenets of the Declaration of Helsinki.

All animal studies were conducted following the Association for Research in Vison and Ophthalmology (ARVO) Statement, Use of Animals in Ophthalmic and Vision Research, and approvals were obtained by Animal Care and Use Committee of Zhongshan Ophthalmic Center.

Author Contributions:

Conception and design: H.Ouyang

Analysis and interpretation: L.Zhu, W.Zhang, J.Zhu, H.Huang, M.Li, H.Ouyang

Data collection: L.Zhu, W.Zhang, J.Zhu, C.Chen, K.Mo, H.Guo, S.Wu, L.Li, J.Tan, Y.Huang, H.Ouyang

Obtained funding: N/A

Overall responsibility: L.Zhu, W.Zhang, J.Zhu, L.Wang, H.Ouyang

Abbreviations and Acronyms:
CEC = corneal epithelial cell; **HAM** = human amniotic membrane; **HGF** = hepatocyte growth factor; **LSC** = limbal stem/progenitor cell; **LSCD** = limbal stem cell deficiency; **LSSC** = limbal stromal stem/progenitor cell; **MSC** = mesenchymal stem cell; **PCA** = principal component analysis; **pLSCD** = post−limbal stem cell deficiency; **α-SMA** = Alpha smooth muscle actin; **SD-OCT** = spectral domain OCT.

Keywords:
Corneal regeneration, Corneal stromal cells, Limbal epithelial cells, Limbal stem cell deficiency, Stem cell-based therapy.

Correspondence:
Hong Ouyang, PhD, State Key Laboratory of Ophthalmology, Zhongshan Ophthalmic Center, Sun Yat-sen University, Guangzhou, 510060, China. E-mail: Ouyhong3@mail.sysu.edu.cn.

References

1. Bonnet C, Gonzalez S, Roberts JS, et al. Human limbal epithelial stem cell regulation, bioengineering and function. *Prog Retin Eye Res*. 2021:100956.
2. Jackson CJ, Erno IT Myklebust, Ringstad H, et al. Simple limbal epithelial transplantation: current status and future perspectives. *Stem Cells Transl Med*. 2020;9:316−327.
3. Yazdanpanah G, Haq Z, Kang K, et al. Strategies for reconstructing the limbal stem cell niche. *Ocul Surf*. 2019;17:230−240.
4. Gabison EE, Huet E, Baudouin C, Menashi S. Direct epithelial-stromal interaction in corneal wound healing: role of EMMPRIN/CD147 in MMPs induction and beyond. *Prog Retin Eye Res*. 2009;28:19−33.
5. Walton KD, Kolterud A, Czerwinski MJ, et al. Hedgehog-responsive mesenchymal clusters direct patterning and emergence of intestinal villi. *Proc Natl Acad Sci U S A*. 2012;109:15817−15822.
6. Daszczuk P, Mazurek P, Pieczonka TD, et al. An intrinsic oscillation of gene networks inside hair follicle stem cells: an additional layer that can modulate hair stem cell activities. *Front Cell Dev Biol*. 2020;8:595178. https://doi.org/10.3389/fcell.2020.595178. eCollection 2020.

7. Wilson SE, Liu JJ, Mohan RR. Stromal-epithelial interactions in the cornea. *Prog Retin Eye Res*. 1999;18:293−309.
8. Wilson SE, Mohan RR, Mohan RR, et al. The corneal wound healing response: cytokine-mediated interaction of the epithelium, stroma, and inflammatory cells. *Prog Retin Eye Res*. 2001;20:625−637.
9. Pinnamaneni N, Funderburgh JL. Concise review: stem cells in the corneal stroma. *Stem Cells*. 2012;30:1059−1063.
10. Lwigale PY, Cressy PA, Bronner-Fraser M. Corneal keratocytes retain neural crest progenitor cell properties. *Dev Biol*. 2005;288:284−293.
11. Du Y, Funderburgh ML, Mann MM, et al. Multipotent stem cells in human corneal stroma. *Stem Cells*. 2005;23:1266−1275.
12. Wilson SE, Marino GK, Torricelli AAM, Medeiros CS. Injury and defective regeneration of the epithelial basement membrane in corneal fibrosis: a paradigm for fibrosis in other organs? *Matrix Biol*. 2017;64:17−26.
13. McTiernan CD, Simpson FC, Haagdorens M, et al. LiQD Cornea: pro-regeneration collagen mimetics as patches and alternatives to corneal transplantation. *Sci Adv*. 2020;6(25): eaba2187. https://doi.org/10.1126/sciadv.aba2187.
14. Kong B, Chen Y, Liu R, et al. Fiber reinforced GelMA hydrogel to induce the regeneration of corneal stroma. *Nat Commun*. 2020;11:1435.
15. Fagerholm P, Lagali NS, Merrett K, et al. A biosynthetic alternative to human donor tissue for inducing corneal regeneration: 24-month follow-up of a phase 1 clinical study. *Sci Transl Med*. 2010;2:46ra61.
16. Funderburgh JL, Funderburgh ML, Du Y. Stem cells in the limbal stroma. *Ocul Surf*. 2016;14:113−120.
17. Basu S, Hertsenberg AJ, Funderburgh ML, et al. Human limbal biopsy-derived stromal stem cells prevent corneal scarring. *Sci Transl Med*. 2014;6:266ra172.
18. Ramilowski JA, Goldberg T, Harshbarger J, et al. A draft network of ligand-receptor-mediated multicellular signalling in human. *Nat Commun*. 2015;6:7866.
19. Ouyang H, Xue Y, Lin Y, et al. WNT7A and PAX6 define corneal epithelium homeostasis and pathogenesis. *Nature*. 2014;511:358−361.
20. Galindo S, Herreras JM, Lopez-Paniagua M, et al. Therapeutic effect of human adipose tissue-derived mesenchymal stem cells in experimental corneal failure due to limbal stem cell niche damage. *Stem Cells*. 2017;35:2160−2174.
21. Bian F, Pelegrino FS, Henriksson JT, et al. Differential effects of dexamethasone and doxycycline on inflammation and MMP production in murine alkali-burned corneas associated with dry eye. *Ocul Surf*. 2016;14:242−254.
22. McCaa CS. The eye and visual nervous system: anatomy, physiology and toxicology. *Environ Health Perspect*. 1982;44: 1−8.
23. Ma DH, Chen JK, Zhang F, et al. Regulation of corneal angiogenesis in limbal stem cell deficiency. *Prog Retin Eye Res*. 2006;25:563−590.
24. Li J, Browning S, Mahal SP, et al. Darwinian evolution of prions in cell culture. *Science*. 2010;327:869−872.
25. Vigneault F, Zaniolo K, Gaudreault M, et al. Control of integrin genes expression in the eye. *Prog Retin Eye Res*. 2007;26:99−161.
26. Roberts ME, Magowan L, Hall IP, Johnson SR. Discoidin domain receptor 1 regulates bronchial epithelial repair and matrix metalloproteinase production. *Eur Respir J*. 2011;37: 1482−1493.
27. Schmassmann A, Stettler C, Poulsom R, et al. Roles of hepatocyte growth factor and its receptor Met during gastric ulcer healing in rats. *Gastroenterology*. 1997;113:1858−1872.
28. Mukhopadhyay M, Gorivodsky M, Shtrom S, et al. Dkk2 plays an essential role in the corneal fate of the ocular surface epithelium. *Development*. 2006;133:2149−2154.
29. Ambati BK, Nozaki M, Singh N, et al. Corneal avascularity is due to soluble VEGF receptor-1. *Nature*. 2006;443: 993−997.
30. Omoto M, Suri K, Amouzegar A, et al. Hepatocyte growth factor suppresses inflammation and promotes epithelium repair in corneal injury. *Mol Ther*. 2017;25:1881−1888.
31. Dunlevy JR, Beales MP, Berryhill BL, et al. Expression of the keratan sulfate proteoglycans lumican, keratocan and osteoglycin/mimecan during chick corneal development. *Exp Eye Res*. 2000;70:349−362.
32. Le Q, Xu J, Deng SX. The diagnosis of limbal stem cell deficiency. *Ocul Surf*. 2018;16:58−69.
33. Rama P, Matuska S, Paganoni G, et al. Limbal stem-cell therapy and long-term corneal regeneration. *N Engl J Med*. 2010;363:147−155.
34. Zhang H, Lin S, Zhang M, et al. Comparison of two rabbit models with deficiency of corneal epithelium and limbal stem cells established by different methods. *Tissue Eng Part C Methods*. 2017;23:710−717.
35. Saika S, Yamanaka O, Okada Y, Sumioka T. Modulation of Smad signaling by non-TGFbeta components in myofibroblast generation during wound healing in corneal stroma. *Exp Eye Res*. 2016;142:40−48.
36. Shukla S, Mittal SK, Foulsham W, et al. Therapeutic efficacy of different routes of mesenchymal stem cell administration in corneal injury. *Ocul Surf*. 2019;17:729−736.
37. Sahu A, Foulsham W, Amouzegar A, et al. The therapeutic application of mesenchymal stem cells at the ocular surface. *Ocul Surf*. 2019;17:198−207.
38. Guo Y, Xue Y, Wang P, et al. Muse cell spheroids have therapeutic effect on corneal scarring wound in mice and tree shrews. *Sci Transl Med*. 2020;12(562):eaaw1120. https://doi.org/10.1126/scitranslmed.aaw1120.
39. Kamil S, Mohan RR. Corneal stromal wound healing: major regulators and therapeutic targets. *Ocul Surf*. 2021;19: 290−306.
40. Ellenberg D, Azar DT, Hallak JA, et al. Novel aspects of corneal angiogenic and lymphangiogenic privilege. *Prog Retin Eye Res*. 2010;29:208−248.
41. Koudouna E, Veronesi G, Patel II, et al. Chemical composition and sulfur speciation in bulk tissue by x-ray spectroscopy and x-ray microscopy: corneal development during embryogenesis. *Biophys J*. 2012;103:357−364.
42. Yu FS, Yin J, Xu K, Huang J. Growth factors and corneal epithelial wound healing. *Brain Res Bull*. 2010;81:229−235.
43. Decline F, Rousselle P. Keratinocyte migration requires alpha2beta1 integrin-mediated interaction with the laminin 5 gamma2 chain. *J Cell Sci*. 2001;114:811−823.